Asociación Argentina
de Mecánica Computacional

Mecánica Computacional Vol XXIX, págs. 5413-5428 (artículo completo)
Eduardo Dvorkin, Marcela Goldschmit, Mario Storti (Eds.)
Buenos Aires, Argentina, 15-18 Noviembre 2010

TRANSIENT HEAT CONDUCTION ANALYSIS USING A BOUNDARY ELEMENT METHOD BASED ON THE CONVOLUTION QUADRATURE METHOD

Ana I. Abreu[a], **Alfredo Canelas**[b] **and Webe J. Mansur**[a]

[a]*Department of Civil Engineering, COPPE/Federal University of Rio de Janeiro, CP 68506, CEP 21945-970, Rio de Janeiro, RJ, Brazil, anai@coc.ufrj.br, webe@coc.ufrj.br*

[b]*Instituto de Estructuras y Transporte, Facultad de Ingeniería, UDELAR, J. Herrera y Ressig 565, CP 11300, Montevideo, Uruguay, acanelas@fing.edu.uy*

Keywords: Transient Heat, Boundary Element Method, Convolution Quadrature Method

Abstract. In this work a fast method for the numerical solution of time-domain boundary integral formulations of transient problems governed by the heat equation is presented. In the formulation proposed, the convolution quadrature method is adopted, i.e., the basic integral equation of the time-domain boundary element method is numerically calculated by a quadrature formula whose weights are computed using the Laplace transform of the fundamental solution. In the case that the responses are required at a large number of interior points, it was observed that the convolution performed to calculate them is very time consuming. In this work it is shown that the discrete convolution can be obtained by means of fast Fourier transform techniques, hence reducing considerably the computational complexity. To validate the numerical techniques studied, results for some transient heat conduction examples are presented.

1 INTRODUCTION

For heat transfer problems, the classical time-domain (TD) formulation of the Boundary Element Method (BEM) presents convolution integrals with respect to the time variable. One of the recognized disadvantages of the classical TD-BEM approach lies in the high computational cost concerning the calculation of the matrices and also the evaluation of the convolution integrals. Besides, in spite of the BEM requires only a surface mesh, when it is used for the analysis of problems with complex-shaped domains, it must solve large linear systems of equations defined by non-symmetric and fully populated matrices.

The BEM has been already used to solve transient heat conduction problems. In the literature, different BEM approaches have been used to address this topic. One approach is by using convolution schemes, where the TD fundamental solution is introduced to state a transient boundary integral equation model (Wrobel, 2002). To make possible such procedures it is necessary to know the TD fundamental solution. Other approach is to define a time-stepping procedure. This approach requires domain integration which, in their turn, can be addressed using the dual reciprocity technique, triple reciprocity technique or similar ones (Tanaka and Chen, 2001; Kassab and Divo, 2006; Erhart et al., 2006; Kassab and Wrobel, 2000; Divo et al., 2003; Ochiai et al., 2006; Divo and Kassab, 1998).

Other alternative approaches to address transient heat problems consist of the use of the Laplace transform and its inverse. Applying the Laplace transform to the TD governing equation it is possible to eliminate the time derivative and solve the problem in the Laplace domain using a steady-state BEM approach (Rizzo and Shippy, 1970; Wrobel, 2002). To recover the real TD solution, the result obtained in the Laplace domain is inverted by means of the inverse Laplace transform. However, due to the fact that the numerical inversion is an ill-posed problem, special methods for the numerical Laplace inversion are required. Among these numerical techniques of inversion, the most commonly used is the Stehfest algorithm (Stehfest, 1970; Kassab and Divo, 2006).

Recently, the Convolution Quadrature Method (CQM) has been found suitable for the application to TD-BEM approaches. This method evaluates the convolution integral of the TD-BEM formulations by mean of a quadrature formula that uses the fundamental solution in the Laplace transformed domain. One of the advantages of using the CQM is that it makes the BEM able for problems where the analytical TD fundamental solution is not available or is difficult to compute.

The CQM was firstly described in (Lubich, 1988a,b; Lubich and Schneider, 1992; Lubich, 1994) and provides a direct procedure to obtain a stable BEM approach that uses the Laplace transform of the TD fundamental solution. Applications of the CQM-Based BEM (a.k.a. CQM-BEM or also convolution quadrature method) to elastodynamics, viscoelasticity and poroelasticity problems can be found in (Schanz, 1972; Messner and Schanz, 2010) and for acoustics in (Abreu et al., 2003, 2006, 2008, 2009). Furthermore, with the aim to accelerate and improve the computational efficiency, it was combined with the multipole method to formulate a CQM-Based BEM for diffraction of waves problems in (Saitoh et al., 2007a,b, 2009).

In the present work, a CQM-Based BEM is used for the TD solution of two-dimensional transient heat conduction problems. In this work it is explained how the discrete convolution of the CQM-Based BEM can be implemented using fast Fourier transform (FFT) technique to reduce the computational cost of the numerical calculation. Results for some transient heat conduction examples are presented to validate the proposed method.

2 DEFINITIONS AND GOVERNING EQUATION

The continuity equation in heat conduction problems is (Özişik, 1993; Carslaw and Jaeger, 1988; Crank, 1975):

$$\frac{\partial u(X,t)}{\partial t} + \nabla \cdot J(X,t) = F(X,t) \quad \text{in } \Omega\,, \tag{1}$$

where u is the internal energy, J is the flux of heat vector, F is the amount of heat per unit volume that is increased (or withdrawal) in the material body Ω of the two-dimensional Euclidean space.

The Fourier law of heat conduction formulates a linear relationship between the flux of heat vector and the gradient of the temperature field T. This constitutive relation for isotropic materials is given by:

$$J(X,t) = -K(X,t)\nabla T(X,t)\,, \tag{2}$$

where $K > 0$ is the thermal conductivity of the material. The relation of specific heat expresses that the variation of internal energy is reflected in the local variation of temperature, i.e.:

$$\frac{\partial u(X,t)}{\partial t} = c(X,t)\rho(X,t)\frac{\partial T(X,t)}{\partial t}\,, \tag{3}$$

where c represents the specific heat of the material, ρ its mass density. For a homogeneous material of constant properties K, c and ρ, Eqs. (1) and (2) applied on Eq. (3) gives:

$$\frac{\partial T(X,t)}{\partial t} - k\nabla^2 T(X,t) = f(X,t)\,, \tag{4}$$

where k is the thermal diffusivity given by $k = K/(c\rho)$ and $f = F/(c\rho)$. Equation (4) is known as the heat equation and describes the evolution of the temperature T inside a homogeneous and isotropic material in the presence of sources of heat given by f. Note that, in this simple model the material properties K, c and ρ do not depend on the time. This assumption is usually accurate when small variation of temperature arises.

The heat conduction problem consists to solve Eq. (4) for the unknown function T. The function f is known, as well as the material properties, the initial condition $T(X,t_0)$ at the initial time t_0 and the following boundary conditions:

$$\begin{aligned} T(X,t) &= \bar{T}(X,t) \quad \text{in } \Gamma_T\,, \\ q(X,t) &= \bar{q}(X,t) \quad \text{in } \Gamma_q\,, \end{aligned} \tag{5}$$

where $q(X,t) = -k\frac{\partial T}{\partial n}(X,t)$, Γ_T and Γ_q are the regions of the boundary Γ of Ω where Dirichlet and Neumann boundary conditions are respectively applied ($\Gamma_T \cup \Gamma_q = \Gamma$). $\bar{T}$ and $\bar{q}$ are known functions and n is the outward unit normal to Γ.

3 CQM-BASED BEM FORMULATION

Assuming a homogeneous initial condition, i.e., $T(X,t_0) = 0$, and null heat sources, Eq. (4) can be formulated into a boundary integral equation of the form (Wrobel, 2002):

$$c(\xi)T(\xi,t) = \int_\Gamma \int_{t_0}^{t_f} T^*(r,t-\tau)q(X,\tau)\,\mathrm{d}\tau\,\mathrm{d}\Gamma - \int_\Gamma \int_{t_0}^{t_f} q^*(r,t-\tau)T(X,\tau)\,\mathrm{d}\tau\,\mathrm{d}\Gamma\,, \tag{6}$$

In Eq. (6), $T^*(r,t-\tau)$ is the TD fundamental solution, $q^*(r,t-\tau)=-k\frac{\partial T^*}{\partial n}(r,t-\tau)$, with $r=|X-\xi|$. The coefficient $c(\xi)=1$ when the source point ξ belongs to the domain Ω and $c(\xi)=\theta/(2\pi)$ when $\xi\in\Gamma$, where θ is the internal angle formed by the left and right tangents to Γ at ξ.

To solve the boundary integral Eq. (6) it is required both space and time discretizations. The BEM represents Γ and the boundary values of T an q by using piece-wise polynomial functions. For this purpose the boundary is divided into J elements Γ_j ($j=1,2,\dots J$). The time discretization consists in dividing the time span $[t_0,t_f]$ into N time-steps of equal size Δt. A discrete version of Eq. (6) using the CQM for a point source ξ and the time $t_n=t_0+n\Delta t$ is given by (Lubich and Schneider, 1992; Abreu et al., 2003, 2006):

$$c(\xi_i)T(\xi_i,t_n)=\sum_{j=1}^{J}\sum_{m=0}^{n}\boldsymbol{g}^j_{n-m}(\xi_i,\Delta t)\boldsymbol{q}^j_m-\sum_{j=1}^{J}\sum_{m=0}^{n}\boldsymbol{h}^j_{n-m}(\xi_i,\Delta t)\boldsymbol{T}^j_m\,,\quad n=0,1,\dots,N\,. \tag{7}$$

The quadrature weights $\boldsymbol{g}_n$ and $\boldsymbol{h}_n$ of Eq. (7) are given by:

$$\boldsymbol{g}^j_n(\xi,\Delta t)=\frac{\sigma^{-n}}{L}\sum_{\ell=0}^{L-1}\int_{\Gamma_j}\hat{T}^*(r,s_\ell)\boldsymbol{N}^j(X)\,\mathrm{d}\Gamma\;e^{-\alpha n\ell}\,, \tag{8}$$

$$\boldsymbol{h}^j_n(\xi,\Delta t)=\frac{\sigma^{-n}}{L}\sum_{\ell=0}^{L-1}\int_{\Gamma_j}\hat{q}^*(r,s_\ell)\boldsymbol{N}^j(X)\,\mathrm{d}\Gamma\;e^{-\alpha n\ell}\,, \tag{9}$$

where the parameter $\alpha=2\pi\mathrm{i}/L\;\left(\mathrm{i}=\sqrt{-1}\right)$.

In the previous expressions, $\boldsymbol{N}^j(X)$ represents the matrix of interpolation functions of the spatial discretization. The discrete parameter $s_\ell=\gamma(\sigma e^{\alpha\ell})/\Delta t$. The function γ is given by:

$$\gamma(z)=\sum_{n=1}^{p}\frac{1}{n}(1-z)^n\,,\quad z\in\mathbb{C}\,, \tag{10}$$

and it is the quotient of the characteristic polynomial generated by a linear multi-step method that is usually a backward differentiation formula of order p (Lubich, 1988a,b).

Setting $L=N$ and $\sigma^N=\sqrt{\varepsilon}$ in Eq. (8) and (9), the quadrature weights $\boldsymbol{g}_n$ and $\boldsymbol{h}_n$ are computed within an error of order $O(\varepsilon)$, where ε is the precision with which $\hat{T}^*(r,s_\ell)$ and $\hat{q}^*(r,s_\ell)$ are calculated (Lubich and Schneider, 1992). $\hat{T}^*(r,\cdot)$ and $\hat{q}^*(r,\cdot)$ are the Laplace transform of $T^*(r,\cdot)$ and $q^*(r,\cdot)$, respectively. The expressions of these fundamental solutions for a heat point source are given by (Morse and Feshbach, 1953; Wrobel, 2002):

$$\hat{T}^*(r,s)=\frac{1}{2\pi k}K_0\left(\sqrt{\frac{s}{k}}\,r\right)\,, \tag{11}$$

$$\hat{q}^*(r,s)=\frac{\partial\hat{T}^*}{\partial r}(r,s)\frac{\partial r}{\partial n}=-\frac{1}{2\pi k}\sqrt{\frac{s}{k}}K_1\left(\sqrt{\frac{s}{k}}\,r\right)\frac{\partial r}{\partial n}\,, \tag{12}$$

where K_ν is the modified Bessel function of the second kind and order ν.

$\boldsymbol{T}^j_m$ and $\boldsymbol{q}^j_m$ of Eq. (7) represent, respectively, the prescribed or unknown nodal values of T and q defined at each element j of the boundary, and are given by ($m=0,1,\dots,N$ in the time):

$$\boldsymbol{T}^j_m=\boldsymbol{T}^j(t_m)=\boldsymbol{T}^j(t_0+m\Delta t)\,, \tag{13}$$

$$\boldsymbol{q}^j_m=\boldsymbol{q}^j(t_m)\;=\boldsymbol{q}^j(t_0+m\Delta t)\,. \tag{14}$$

Equation (7) can be rewritten in matrix form as follows:

$$\boldsymbol{c}\boldsymbol{T}^n = \sum_{m=0}^{n} \boldsymbol{G}^{n-m}\boldsymbol{q}^m - \sum_{m=0}^{n} \boldsymbol{H}^{n-m}\boldsymbol{T}^m \,. \tag{15}$$

The responses on the boundary and at interior points are calculated from Eq. (15), where $\boldsymbol{G}$ and $\boldsymbol{H}$ are the BEM influence matrices and $\boldsymbol{c}$ is the diagonal matrix containing the coefficients $c(\xi)$. The indices n and m correspond to the discrete times $t_n = t_0 + n\Delta t$ and $t_m = t_0 + m\Delta t$, respectively. To compute the responses on the boundary, the boundary conditions have to be imposed into Eq. (15). The following general expression is obtained:

$$\boldsymbol{A}^0\boldsymbol{y}^n = \boldsymbol{f}^n + \sum_{m=0}^{n-1} \left(\boldsymbol{G}^{n-m}\boldsymbol{q}^m - \boldsymbol{H}^{n-m}\boldsymbol{T}^m\right) \,, \tag{16}$$

where $\boldsymbol{A}^0$ stores the columns of $\boldsymbol{c} + \boldsymbol{H}^0$ corresponding to the unknown values of $\boldsymbol{T}$ and the columns of $\boldsymbol{G}$ corresponding to the unknowns values of $\boldsymbol{q}$. The unknown values of $\boldsymbol{T}$ and $\boldsymbol{q}$ at time t_n are stored in the vector $\boldsymbol{y}_n$. The known values of $\boldsymbol{T}$ and $\boldsymbol{q}$ are multiplied for their respective columns of $\boldsymbol{H}$ and $\boldsymbol{G}$ to assemble the vector $\boldsymbol{f}_n$.

From Eq. (16) it is possible to observe that the linear systems that the method solves to obtain the unknown vectors $\boldsymbol{y}_n$ have all the same coefficient matrix $\boldsymbol{A}^0$. Thus, the method needs of just one factorization. The other influence matrices are used only for the computation of the independent terms.

3.1 Computation of the influent matrices

It was observed that most of the computational cost of solution is due to the computation and storage of the influent matrices, and also due to the numerical convolution. These two tasks can be studied separately. In this section it will be explained how to compute and assemble the influent matrices in order to reduce the computational cost.

The quadrature weights $\boldsymbol{g}_n$ and $\boldsymbol{h}_n$ can be obtained efficiently using the FFT algorithm (Cooley and Tukey, 1965; Brigham, 1988): examining the expressions of the quadrature weights and, taking into consideration the definition of the discrete Fourier transform (DFT), Eqs. (8) and (9) can be rewritten in the following form:

$$\boldsymbol{g}_n^j(\xi, \Delta t) = \frac{\sigma^{-n}}{L} \sum_{\ell=0}^{L-1} \hat{\boldsymbol{T}}_\ell^{*j} e^{-\alpha n \ell} \,, \tag{17}$$

$$\boldsymbol{h}_n^j(\xi, \Delta t) = \frac{\sigma^{-n}}{L} \sum_{\ell=0}^{L-1} \hat{\boldsymbol{q}}_\ell^{*j} e^{-\alpha n \ell} \,. \tag{18}$$

where $\hat{\boldsymbol{T}}_\ell^{*j}$ and $\hat{\boldsymbol{q}}_\ell^{*j}$ are:

$$\hat{\boldsymbol{T}}_\ell^{*j} = \int_{\Gamma_j} \hat{T}^*(r, s_\ell)\boldsymbol{N}^j(X)\,\mathrm{d}\Gamma \,, \tag{19}$$

$$\hat{\boldsymbol{q}}_\ell^{*j} = \int_{\Gamma_j} \hat{q}^*(r, s_\ell)\boldsymbol{N}^j(X)\,\mathrm{d}\Gamma \,. \tag{20}$$

Thus, to obtain $\boldsymbol{g}_n$ and $\boldsymbol{h}_n$ it is enough to calculate the FFT transform of $\hat{\boldsymbol{T}}_\ell^*$ and $\hat{\boldsymbol{q}}_\ell^*$ and multiply the results by the factor σ^{-n}/L. Using the FFT algorithms one quadrature weight can be

obtained with a number of operations the order $N\log(N)$, keeping in mind that $N = L$. The element integrals should be performed before the FFT in order to reduce the number of times that the FFT routine is called; otherwise, when using the Gauss quadrature formula one would have to call the FFT routine once for each Gauss point.

3.2 Discrete convolution for interior points

As mentioned before, the numerical convolution is one of the most expensive tasks, if not the most, of those performed by the CQM-Based BEM, mainly in the case where the responses at a large number of interior points are required. This section describes how the numerical convolution is implemented in order to reduce the computational cost. Consider the following notations:
J: Number of elements used to discretize the boundary;
$Nnod$: Number of nodes;
Nip: Number of interior points where the numerical response is calculated;
N: Number of time-steps (that also represents the number of Fourier coefficients).

It is ease to see that the right hand side of Eq. (15) results in a block triangular Toeplitz matrix, i.e., a matrix in which each descending diagonal from left to right has constant values. Consider the following equation:

$$\boldsymbol{y}_n = \sum_{j=0}^{N} \boldsymbol{a}_{n-j}\boldsymbol{x}_j\,, \quad 0 \le n \le N\,, \tag{21}$$

where $\boldsymbol{y} \in \mathbb{R}^{N+1}$, $\boldsymbol{a} \in \mathbb{R}^{N+1}$, $\boldsymbol{x} \in \mathbb{R}^{N+1}$ and $a_j = a_{N+1+j}$ for a negative index j. Eq. (21) is the expansion of the discrete convolution $\boldsymbol{y} = \boldsymbol{a} * \boldsymbol{x}$. Alternatively, $\boldsymbol{y}$ can be calculated by the product $\boldsymbol{y} = \boldsymbol{A}\boldsymbol{x}$ where the circulant matrix $\boldsymbol{A}$ has coefficients $A_{ij} = a_{i-j}$. The convolution of Eq. (21) can also be computed as (Brigham, 1988):

$$\boldsymbol{y} = \mathcal{F}^{-1}\left(\mathcal{F}(\boldsymbol{a}) \circ \mathcal{F}(\boldsymbol{x})\right)\,, \tag{22}$$

where the notation $\mathcal{F}(\cdot)$ means discrete Fourier transform, $\mathcal{F}^{-1}(\cdot)$ is the inverse discrete Fourier transform and the symbol "$\circ$" denotes the Hadamard product of vectors $(\boldsymbol{a} \circ \boldsymbol{x})_i = \boldsymbol{a}_i\boldsymbol{b}_i$. Therefore, the vector $\boldsymbol{y}$ can be calculated efficiently using the FFT algorithm with a number of operations of order $3N\log(N)$ (three calls to the FFT algorithm).

Consider now the following equation:

$$\boldsymbol{y}_n = \sum_{j=0}^{n} \boldsymbol{a}_{n-j}\boldsymbol{x}_j\,, \quad 0 \le n \le N\,. \tag{23}$$

Equation (23) it is not a convolution in the form of Eq. (21) because the upper limit of the sum is not equal than the upper limit of the sum of Eq. (21). However, if the vectors $\boldsymbol{a}$ and $\boldsymbol{x}$ are extended in the form:

$$\begin{cases} \boldsymbol{a}^j = 0\,, & N+1 \le j \le 2N\,, \\ \boldsymbol{x}^j = 0\,, & N+1 \le j \le 2N\,, \end{cases} \tag{24}$$

then

$$\boldsymbol{y}_n = \sum_{j=0}^{2N} \boldsymbol{a}_{n-j}\boldsymbol{x}_j\,, \quad 0 \le n \le N\,. \tag{25}$$

The vector $\boldsymbol{y}$ in its turn can be extended in order to obtain a convolution in the form of Eq. (21):

$$\boldsymbol{y}_n = \sum_{j=0}^{2N} \boldsymbol{a}_{n-j}\boldsymbol{x}_j\,, \quad 0 \le n \le 2N\,. \tag{26}$$

Therefore, using the FFT algorithm, $\boldsymbol{y}$ can be obtained in $(6N)\log(2N)$ operations.

For interior points, Eq. (7) with $c(\xi) = 1$ gives:

$$T(\xi, t_n) = \sum_{j=1}^{J}\sum_{m=0}^{n} \boldsymbol{g}^j_{n-m}(\xi, \Delta t)\boldsymbol{q}^j_m - \sum_{j=1}^{J}\sum_{m=0}^{n} \boldsymbol{h}^j_{n-m}(\xi, \Delta t)\boldsymbol{T}^j_m\,,\ n = 0, 1, \ldots, N\,, \tag{27}$$

which can be expressed as:

$$T(\xi, t_n) = \sum_{j=1}^{J} \boldsymbol{G}^j_n - \sum_{j=1}^{J} \boldsymbol{H}^j_n\,,\ n = 0, 1, \ldots, N\,, \tag{28}$$

with $\boldsymbol{G}^j_n$ and $\boldsymbol{H}^j_n$ defined as:

$$\boldsymbol{G}^j_n = \sum_{m=0}^{n} \boldsymbol{g}^j_{n-m}(\xi, \Delta t)\boldsymbol{q}^j_m\,, \tag{29}$$

$$\boldsymbol{H}^j_n = \sum_{m=0}^{n} \boldsymbol{h}^j_{n-m}(\xi, \Delta t)\boldsymbol{T}^j_m\,. \tag{30}$$

Matrices $\boldsymbol{G}^j_n$ and $\boldsymbol{H}^j_n$ can be obtained efficiently using the FFT algorithm in the same way as $\boldsymbol{y_n}$ of Eq. (23). Thus, each component of $\boldsymbol{G}^j_n$ and $\boldsymbol{H}^j_n$ is obtained in $(6N)\log(2N)$ operations. Therefore, for the interior point ξ, $T(\xi, t_n)$ of Eq. (27) can be obtained in $(12JN)\log(2N)$ operations. Then, the total number of operations to obtain the responses at Nip interior points is of the order $(12JNNip)\log(2N)$ plus the operations required to compute all the element matrices $\boldsymbol{g}^j_n$ and $\boldsymbol{h}^j_n$.

4 NUMERICAL EXAMPLES

To validate the proposed method, some examples considering three different domains are analyzed. The numerical responses of transient heat conduction problems for these examples were compared to the analytical responses (Carslaw and Jaeger, 1988; Özişik, 1993; Crank, 1975). All the examples share the following characteristics:

- It was taken $L = N$ and $\sigma^N = \sqrt{\varepsilon}$ with $\varepsilon = 10^{-4}$.
- The time-step Δt is fixed (it is an inherent feature of the CQM).
- It was taken $\gamma(z) = \frac{3}{2} - 2z + \frac{1}{2}z^2$ (corresponding to a backward differentiation formula of order $p = 2$).
- Lineal elements were used for the spatial discretization.
- Uniform initial condition, i.e., $T(X, t_0) = T_0$. The particular solution $T(X, t) = T_0$ was used to solve zero initial condition examples.
- Zero heat sources (homogeneous equation).

4.1 Circular region

In this example the transient heat conduction analysis inside a circular region of radius $R = 1.0$ mm is considered. A constant Dirichlet boundary condition (DBC) $\bar{T}(r,t)|_{r=R} = 0.0\,^{\circ}$C, is prescribed. The initial condition is $T(X,t_0) = T_0$, with $T_0 = 1.0\,^{\circ}$C. The geometry of the region of this example is depicted in Fig. 1.

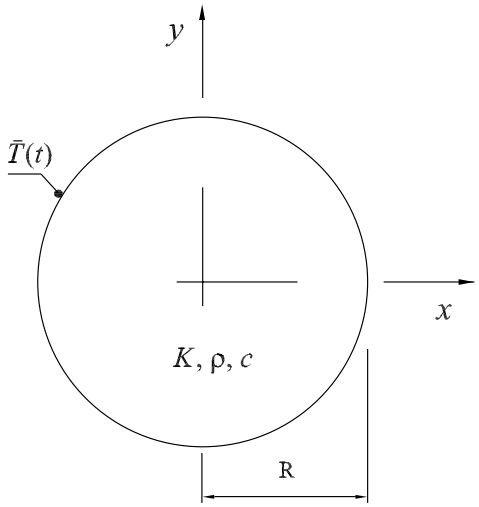

Figure 1: Circular region: geometry and boundary condition.

The thermal diffusivity is $k = 1.0\,\text{mm}^2/\text{s}$. A boundary mesh of $J = 48$ elements was used. A time interval from $t_0 = 0.0$ s to $t_f = 0.5$ s is analyzed. For the time discretization, two cases were tested. The first case corresponds to 32 time-steps of $\Delta t = 0.0156$ s. The second case corresponds to 1024 time-steps of $\Delta t = 0.0005$ s. Figure 2 shows the evolution of the temperature at point A located in the center of the circular region. The figure shows that the responses are accurate when compared with the exact solution. The temperature field on the horizontal diameter of the circular region for the time $t = 0.25$ s is shown in Fig. 3.

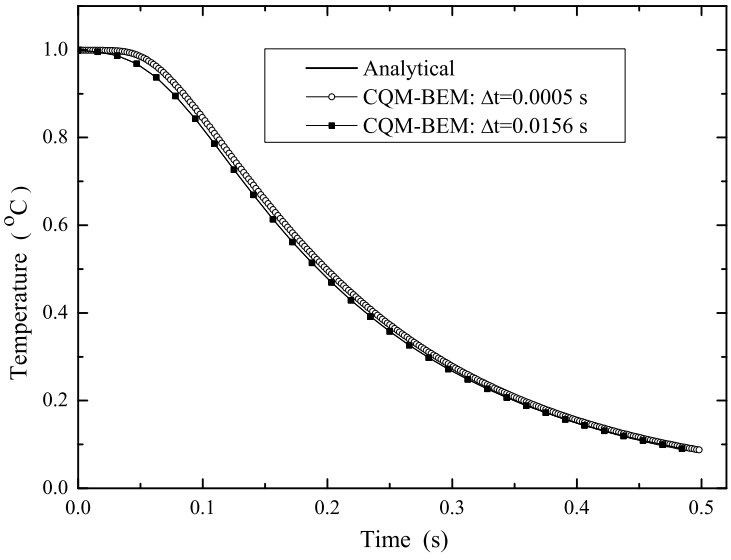

Figure 2: Evolution of the temperature at point A of the circular region with DBC.

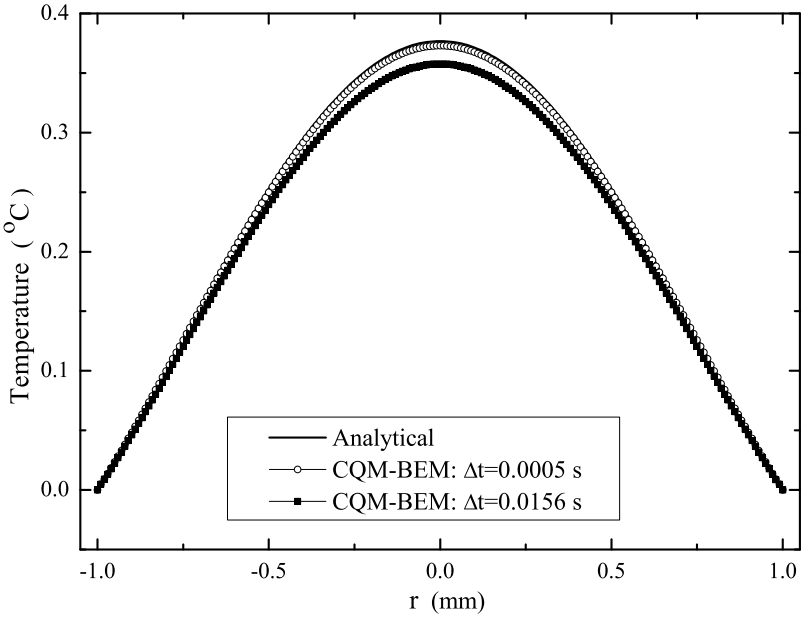

Figure 3: Temperature at time $t = 0.25$ s on the horizontal diameter of the circular region with DBC.

Figures 4 and 5 show the results obtained for the same circular region subject to Neumann boundary conditions (NBC) corresponding to a flux $\bar{q}(r,t)|_{r=R} = -1.0\,°$Cmm/s.

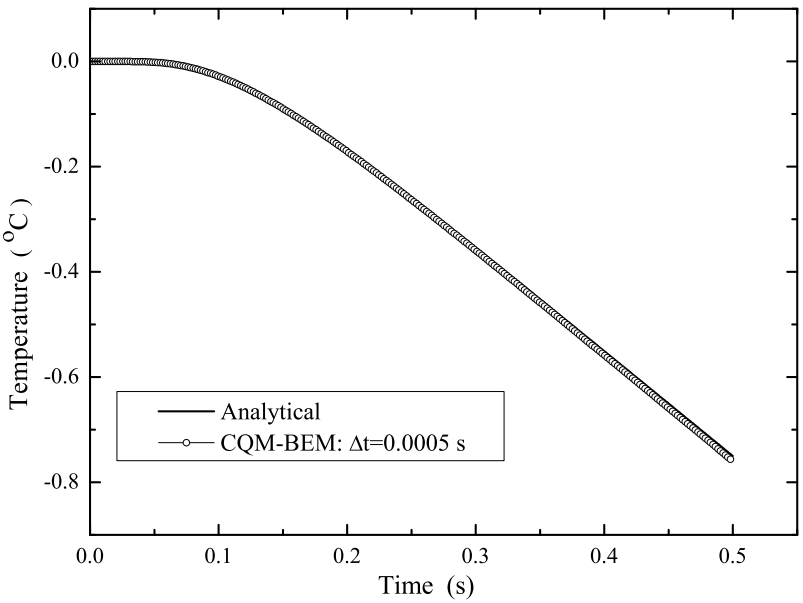

Figure 4: Evolution of the temperature at point A of the circular region with NBC.

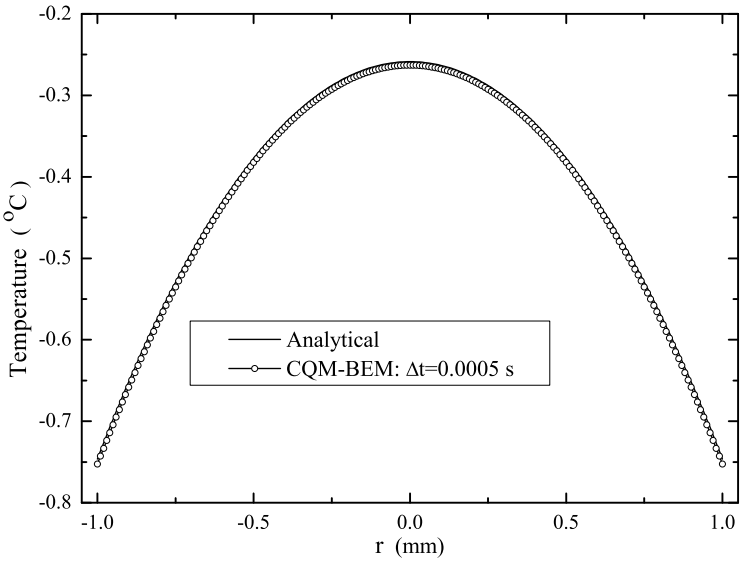

Figure 5: Temperature at time $t = 0.25$ s on the horizontal diameter of the circular region with NBC.

The next example considers a circular region of radius $R = 10.0$ mm. The initial condition is $T(X, t_0) = 0.0\,^{\circ}$C. The thermal diffusivity is $k = 4.0\,\text{mm}^2/\text{s}$. A boundary mesh of $J = 48$ elements was used. A time interval from $t_0 = 0.0$ s to $t_f = 20.0$ s is analyzed. The time discretization consists of 2048 time-steps of $\Delta t = 0.00977$ s. Dirichlet harmonic boundary condition (DHBC) was prescribed. The expression of this boundary condition is given by:

$$T(r,t)|_{r=R} = T_0(1 - \cos(\omega t))\,, \tag{31}$$

with $T_0 = 10.0°$C and $\omega = \pi/2$ rad/s.

Figure 6 shows the evolution of the temperature at two interior points of coordinates $(x, y) = (0.0, 0.0)$ and $(x, y) = (8.0, 0.0)$. Figure 7 shows the temperature at time $t = 10.0$ s on the horizontal diameter of the circular region.

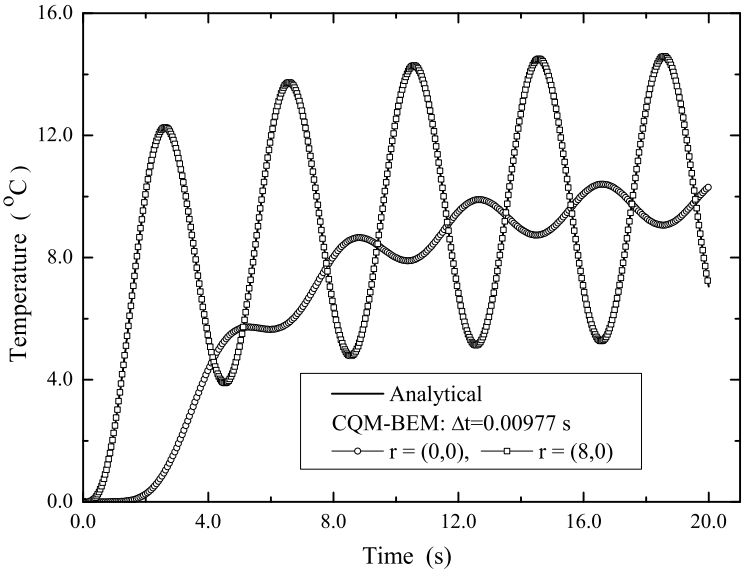

Figure 6: Evolution of the temperature at two interior points of the circular region with DHBC.

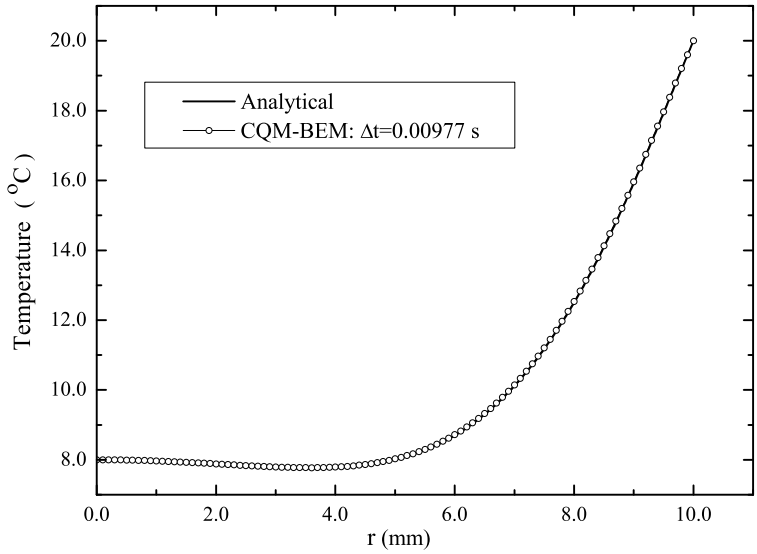

Figure 7: Temperature at time $t = 10.0\,\text{s}$ on the horizontal diameter of the circular region with DHBC.

4.2 One-dimensional rod

This example considers the transient heat conduction problem inside a one-dimensional rod of size $L \times L/2$, where $L = 2.0$ mm, as depicted in Fig. 8. The example considers mixed Dirichlet and Neumann boundary conditions: the sides of length L are thermally isolated, the lateral sides of length $L/2$ are subject to the temperature $\bar{T}(t) = 0.0°\text{C}$. The initial condition is $T(X, t_0) = T_0$, with $T_0 = 1.0\,°\text{C}$.

The thermal diffusivity $k = 1.0$ mm^2/s was assumed. A boundary mesh of $J = 76$ elements was used. A time interval from $t_0 = 0.0\,\text{s}$ to $t_f = 0.5\,\text{s}$ is analyzed. The time discretization consist of 1024 time-steps of length $\Delta t = 0.0005\,\text{s}$.

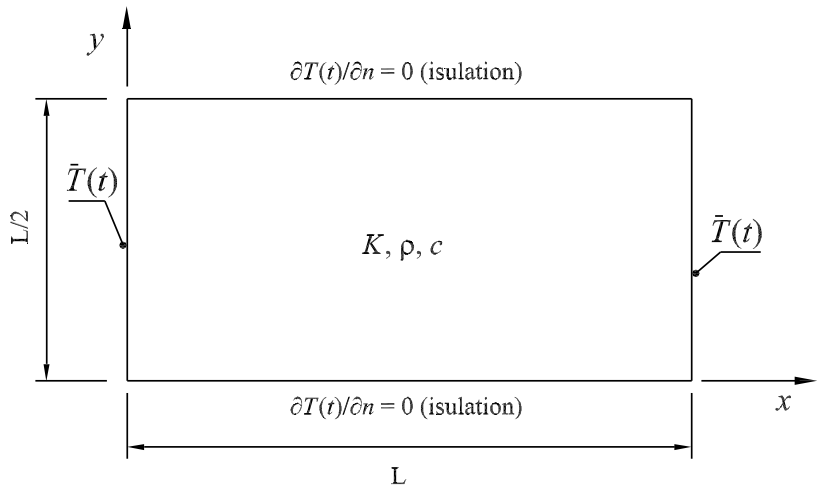

Figure 8: One-dimensional rod: geometry and mixed boundary conditions.

The evolution of the temperature at the center point $C = (1.0, 0.5)$ is shown in Fig. 9. The figure shows that the numerical responses obtained using the CQM-based BEM are in good

agreement with the exact solution. The temperature at time $t = 0.25\,\text{s}$ on the horizontal axis of the rod is shown in Fig. 10.

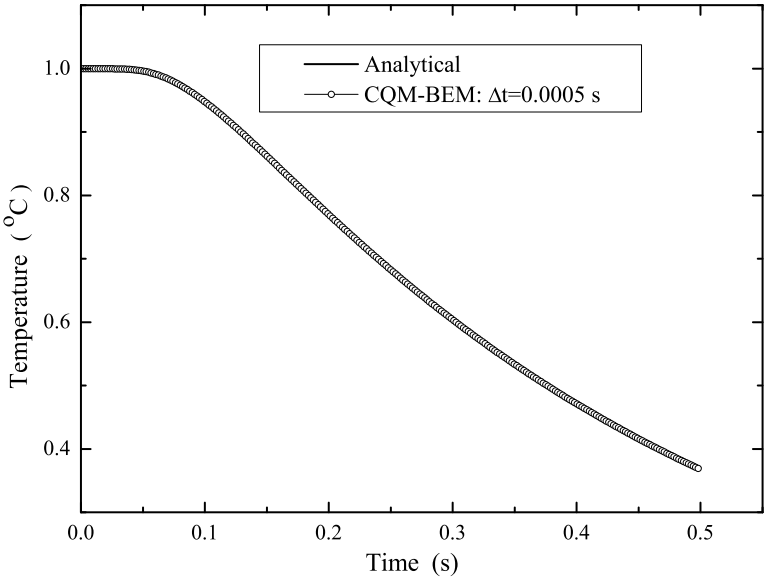

Figure 9: Evolution of the temperature at node C of the one-dimensional rod.

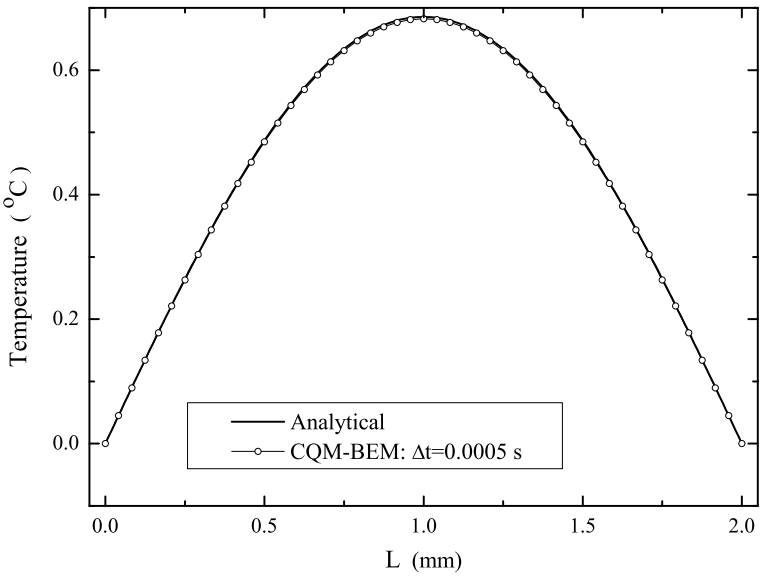

Figure 10: Temperature at time $t = 0.25\,\text{s}$ on the horizontal axis of the one-dimensional rod.

4.3 Square region

This example considers the analysis of the transient heat conduction inside a square region of dimension $L \times L$, where $L = 100.0$ mm as specified in Fig. 11. The horizontal sides are thermally isolated and the right side is subject to the temperature $\bar{T}(t) = 0.0°\text{C}$. The left side considers DHBC given by Eq. (31), with $T_0 = 10.0\,°\text{C}$ and $\omega = \pi/100$ rad/s. The initial condition is $T(X, t_0) = 0.0\,°\text{C}$ and the thermal diffusivity is $k = 16.0\ \text{mm}^2/\text{s}$.

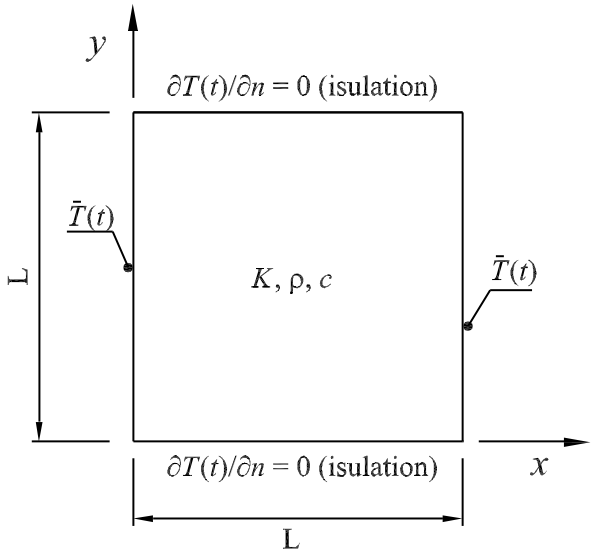

Figure 11: Square region: geometry and boundary conditions.

A boundary mesh of $J = 76$ elements was used. A time interval from $t_0 = 0.0\,\text{s}$ to $t_f = 400.0\,\text{s}$ is analyzed. The time discretization consists of 1024 time-steps of $\Delta t = 0.39\,\text{s}$. Figure 12 shows the evolution of the temperature at two interior points of coordinates $(x, y) = (9.0, 50.0)$ and $(x, y) = (49.0, 50.0)$. Figure 13 shows the temperature at time $t = 200.0\,\text{s}$ on the horizontal axis of the square.

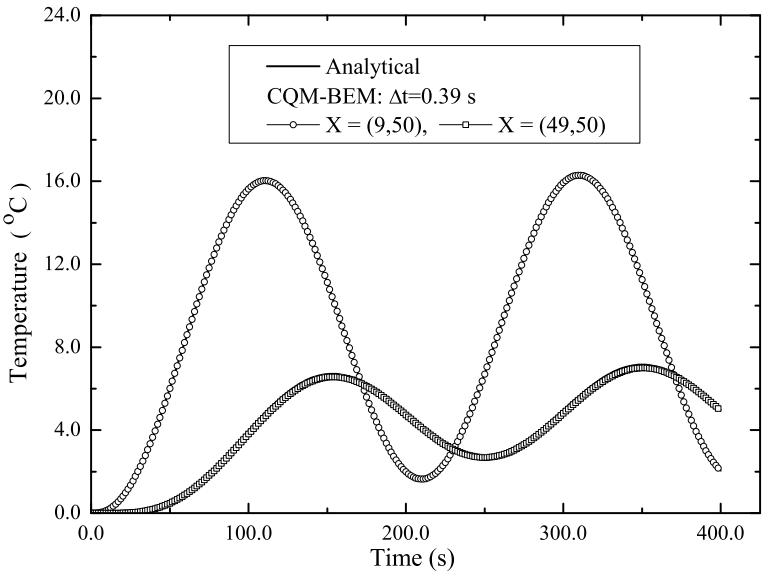

Figure 12: Evolution of the temperature at interior points of the square region with DHBC.

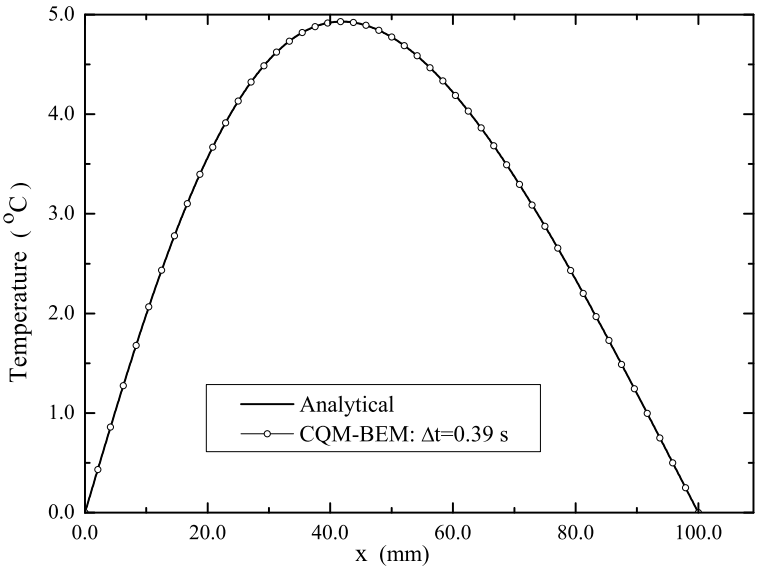

Figure 13: Temperature at time $t = 200.0\,\text{s}$ on the horizontal axis of the square region with DHBC.

5 CONCLUSIONS

A CQM-based BEM formulation was proposed with the purpose of analyzing two-dimensional problems governed by the heat equation. The CQM is an attractive method for the time discretization of the convolution integrals of the time-domain BEM. Interesting characteristics of this approach are: first, the fundamental solution in the Laplace domain is used instead of the fundamental solution in the time-domain; second, the CQM requires the definition of the time-step size Δt only. Other methods that work directly in the Laplace transformed domain need a carefully definition of several parameters to obtain accurate results.

Regarding to the computation cost of the implementation, two important conclusions are achieved:

1. When computing the influent matrices of the BEM the FFT algorithm can be used to reduce the number of operations. Unfortunately, to solve the boundary problem, the cost of the convolution and the cost of storage is high: the FFT cannot be used and a complete storage of the influent matrices is required.

2. For the numerical responses at interior points the method is cheap in the number of operations and storage: the convolution can be computed by using the FFT, and the memory required is related to the element matrices for just one interior point, since the computations for different interior points are complete independent.

The examples analyzed shown that the proposed formulation is accurate and exhibits a stable behavior with respect to the parameter Δt, thus the CQM-Based BEM is well suited for general problems of transient heat conduction.

ACKNOWLEDGMENTS

The authors would like to thank the National Council for Scientific and Technological Development (CNPq) of Brazil and the National Research and Innovation Agency (ANII) of Uruguay for the financial support.

REFERENCES

Abreu A.I., Carrer J.A.M., and Mansur W.J. Scalar wave propagation in 2D: A BEM formulation based on the operational quadrature method. *Engineering Analysis with Boundary Elements*, 27(2):101–105, 2003.

Abreu A.I., Mansur W.J., and Canelas A. Computation of time and space derivatives in a CQM-based BEM formulation. *Engineering Analysis with Boundary Elements*, 33(3):314–321, 2009.

Abreu A.I., Mansur W.J., and Carrer J.A.M. Initial conditions contribution in a BEM formulation based on the convolution quadrature method. *International Journal for Numerical Methods in Engineering*, 67(3):417–434, 2006.

Abreu A.I., Mansur W.J., Spares Jr. D., and Carrer J.A.M. Numerical computation of space derivatives by the complex-variable-differentiation method in the convolution quadrature method based BEM formulation. *CMES. Computer Modeling in Engineering and Sciences*, 30(3):123–132, 2008.

Brigham E.O. *The Fast Fourier Transform and Its Applications*. Signal processing series. Prentice-Hall, 1988.

Carslaw H.S. and Jaeger J.C. *Conduction of heat in solids*. Oxford Science Publications. The Clarendon Press Oxford University Press, New York, second edition, 1988.

Cooley J.W. and Tukey J.W. An algorithm for the machine calculation of complex Fourier series. *Mathematics of Computation*, 19(90):297–301, 1965.

Crank J. *The mathematics of diffusion*. Clarendon Press, Oxford, second edition, 1975.

Divo E. and Kassab A.J. Generalized boundary integral equation for transient heat conduction in heterogeneous media. *Journal of Thermophysics and Heat Transfer*, 12(3):364–373, 1998.

Divo E., Kassab A.J., and Rodriguez F. Parallel domain decomposition approach for large-scale three-dimensional boundary-element models in linear and nonlinear heat conduction. *Numerical Heat Transfer, Part B: Fundamentals*, 44(5):417–437, 2003. Cited By (since 1996) 18.

Erhart K., Divo E., and Kassab A.J. A parallel domain decomposition boundary element method approach for the solution of large-scale transient heat conduction problems. *Engineering Analysis with Boundary Elements*, 30(7):553–563, 2006.

Kassab A.J. and Divo E.A. Parallel domain decomposition boundary element method for large-scale heat transfer problems. In *Integral methods in science and engineering*, pages 117–135. Birkhäuser Boston, Boston, MA, 2006.

Kassab A.J. and Wrobel L.C. Boundary element methods in heat conduction. In W.J. Mincowycz and E.M. Sparrow, editors, *Recent Advances in Numerical Heat Transfer*, volume 2, chapter 5, pages 143–188. Taylor & Francis, 2000.

Lubich C. Convolution quadrature and discretized operational calculus. I. *Numerische Mathematik*, 52(2):129–145, 1988a.

Lubich C. Convolution quadrature and discretized operational calculus. II. *Numerische Mathematik*, 52(4):413–425, 1988b.

Lubich C. On the multistep time discretization of linear initial-boundary value problems and their boundary integral equations. *Numerische Mathematik*, 67(3):365–389, 1994.

Lubich C. and Schneider R. Time discretization of parabolic boundary integral equations. *Numerische Mathematik*, 63(1):455–481, 1992.

Messner M. and Schanz M. An accelerated symmetric time-domain boundary element formulation for elasticity. *Engineering Analysis with Boundary Elements*, 34(11):944–955, 2010.

Morse P.M. and Feshbach H. *Methods of theoretical physics. 2 volumes*. McGraw-Hill Book Co., Inc., New York, 1953.

Ochiai Y., Sladek V., and Sladek J. Transient heat conduction analysis by triple-reciprocity boundary element method. *Engineering Analysis with Boundary Elements*, 30(3):194–204, 2006.

Özişik M.N. *Heat Conduction*. Wiley-Interscience, 2 edition, 1993.

Rizzo F.J. and Shippy D.J. Method of solution for certain problems of transient heat conduction. *AIAA Journal*, 8(11):2004–2009, 1970.

Saitoh T., Hirose S., and Fukui T. Application of fast multipole boundary element method to multiple scattering analysis of acoustic and elastic waves. In *AIP Conference Proceedings*, volume 894, pages 79–86. 2007a.

Saitoh T., Hirose S., and Fukui T. Convolution quadrature time-domain boundary element method and acceleration by the fast multipole method in 2-D viscoelastic wave propagation. *Theoretical and Applied Mechanics Japan*, 57:385–393, 2009.

Saitoh T., Hirose S., Fukui T., and Ishida T. Development of a time-domain fast multiple BEM based on the operational quadrature method in a wave propagation problem. In *Advances in Boundary Elemements Techniques*, volume VIII, pages 355–360. 2007b.

Schanz M. *Wave propagation in viscoelastic and poroelastic continua: A boundary element approach*, volume II of *Lecture Notes in Applied Mechanics*. Springer-Verlag, Berlin, Heidelberg, New York, 1972.

Stehfest H. Numerical inversion of Laplace transforms. *Communications of the ACM*, 13(1):47–49, 1970.

Tanaka M. and Chen W. Coupling dual reciprocity BEM and differential quadrature method for time-dependent diffusion problems. *Applied Mathematical Modelling*, 25(3):257–268, 2001.

Wrobel L.C. *The Boundary Element Method: Applications in Thermo-Fluids and Acoustics*, volume 1. John Wiley & Sons, 2002.